9th Biennial International Conference
& Exposition on Petroleum Geophysics

"HYDERABAD 2012"

P-014

Effects of VTI Anisotropy in Shale-Gas Reservoir Characterization

Niranjan Banik* and Mark Egan, *WesternGeco*

Summary

Shale reservoirs are one of the hottest plays in the oil industry today. Our understanding of these reservoirs rapidly progressed from one of a continuous type, to that of a spatially varying type. Two key elastic parameters, Young's modulus and Poisson's ratio are critically relied upon, to seismically high-grade these spatially varying reservoirs in terms of their reservoir and completion quality. Isotropic elastic properties are assumed in the estimation of "frac'ability' and sweet spots. However, these shale formations are highly anisotropic even in the absence of any in-situ fractures and there are multiple Young's moduli and Poisson's ratios in an anisotropic medium.

In this paper we discuss the effects of vertical transverse isotropy (VTI) in characterizing shale reservoirs in terms of Young's moduli and Poisson's ratios. We linearize Young's modulus and Poisson's ratio expressions in terms of Thomsen's anisotropy parameters (Thomsen, 1986). Exact expressions available in the literature (See, for example, Sayers, 2010) are in terms of transcendental equations, can be understood only through numerical analysis, which is provided in this paper. Approximate expressions are easier to understand. The results are compared with those of the exact expressions. Relevant ranges of values of the anisotropy parameters are used for this comparison. Also, an important contribution to fracture initiation and containment comes from the uniaxial stress ratio (Higgins et al., 2008; Sayers, 2010). It is the ratio of the horizontal to the vertical stress in the absence of any transverse strain. The effects of anisotropy on the uniaxial stress ratio are discussed in this context. Finally we discuss how P-wave surface seismic data can be integrated with borehole and other measurements to estimate relevant elastic attributes in these highly anisotropic shale formations. An integrated seismic inversion scheme for a VTI medium is proposed.

Introduction

The successes with shale reservoirs in the Barnett, Haynesville, Eagle Ford, and other basins in the USA (Figure 1) have encouraged shale gas exploration in other parts of the world. The key technology advancements attributed to this success are horizontal drilling and hydraulic fracturing. In spite of these advances, at current gas prices, the production cost in these unconventional reservoirs is prohibitively high. One main reason is reservoir heterogeneity--nearly 70% of production comes from roughly 30% of "frac" stages. Fracture stages must be optimized.

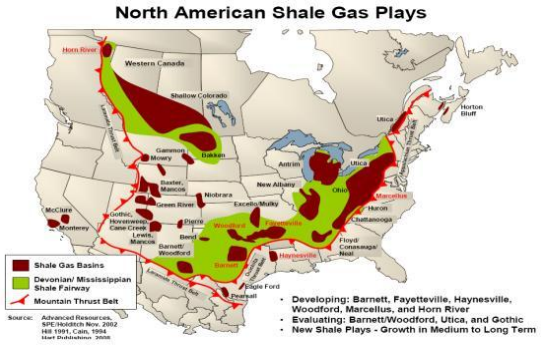

Figure 1: Shale reservoirs in the USA.

Traditionally Poisson's ratio is used to identify sweet spots in conventional gas-sand reservoirs. The Poisson's ratio and the Young's modulus together determine the fracture pressure and fracture extent. Low Poisson's ratio and high Young's modulus make good fracture locations. Surface seismic data allow identifying sweet spots and "-frac'able" zones through estimation of Poisson's ratio and Young's modulus in shale (Banik, et al., 2010 and references therein). Current estimations are based on

WesternGeco, Houston, Texas, USA
Email: NBanik@slb.com

isotropic shale formation. Poststack and prestack inversion provides reasonable estimations of isotropic Poisson‘s ratio and Young‘s modulus. However, these Cretaceous and earlier- age shales are highly anisotropic (Jones and Wang, 1981; Banik, 1984; Sayers 2010).

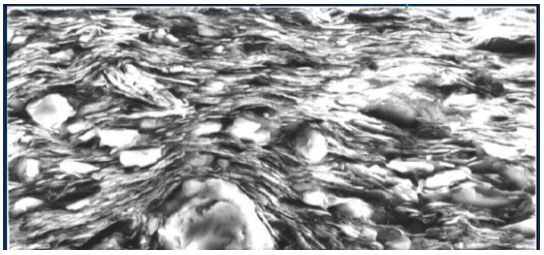

Figure 2: SEM of North Sea Kimmeridgian shale (Schlumberger Cambridge Research,Hornby, 1994). The P-wave velocity anisotropy in this shale is high ~30%.

Scanning electron micrographs such as shown in figure 2 by Hornby (1994) for the North Sea Kimmeridgian shale reveal that clay platelets form a general horizontal pattern while the grain particles are isolated and imbedded in the shale matrix. This kind of formation is described in terms of transverse isotropy with the axis of symmetry as the vertical axis, normal to the bedding plane (VTI). In the presence of dipping formations, the azimuth and the dip angle of the axis of symmetry must be considered.

In this paper we consider shale to be of VTI anisotropy and describe its elastic properties in terms of five elastic parameters. The anisotropic expressions for Young‘s moduli and Poisson‘s ratios are given in the literature in terms of the rock‘s stiffness coefficients C_{ij} in the conventional two-index Voigt notation. For seismic applications, we rewrite these expressions in terms of the well-known Thomsen‘s VTI anisotropy parameters δ, ε, and γ. Both exact and approximate expressions are given in the next section. The results are then discussed with respect to known ranges of these anisotropy parameters as obtained through laboratory measurements of shale samples and also in borehole sonic scanner data.

Anisotropic Young’s moduli and Poisson’s ratios

In isotropic solids, there is only one Young‘s modulus, E_0, and one Poisson‘s ratio, v_0. These are given by

$$E_0 = 2Is^2 (1 + v_0) / \rho. \quad (1)$$

$$v_0 = 0.5 (Ip^2 - 2Is^2) / (Ip^2 - Is^2). \quad (2)$$

Here I_P, I_S, and ρ are the formation‘s acoustic and shear impedances, and bulk density respectively and they can be estimated from good-quality seismic data through prestack seismic inversion. It turns out that the isotropic Young‘s modulus can be also estimated from the acoustic impedance alone in low-porosity formations, as shown in Banik et al. (2010). This is possible because the low-porosity formation is matrix-supported rather than being grain-supported.

In a VTI medium, there are five independent elastic parameters. With x3-axis as the axis of symmetry and using a right-handed coordinate system (Figure 2), the independent stiffness coefficients are C11, C33, C13, C44=C55, and C66 or C12 (see, for example Mavko et al., 2009 or Sayers, 2010). In this paper we use C66 as the fifth stiffness parameter and write C12 = C11 - 2C66.

In such a medium, there are two Young‘s moduli and three Poisson‘s ratios. In terms of C_{ij} they are given by

$$E_{33} = C_{33} - 2C_{13}^2 / (C_{11} + C_{12}) \quad (3)$$

$$E_{11} = C_{11} + \{(C_{13}^2 (C_{12} - C_{11}) + C_{12} (C_{13}^2 - C_{12} C_{33})\} / (C_{33} C_{11} - C_{13}^2) \quad (4)$$

$$v_{31} = v_{32} = C_{13} / (C_{11} + C_{12}) \quad (5)$$

$$v_{13} = v_{23} = C_{13} (C_{11} - C_{12}) / (C_{33} C_{11} - C_{13}^2) \quad (6)$$

$$v_{12} = v_{21} = (C_{33} C_{12} - C_{13}^2) / (C_{33} C_{11} - C_{13}^2) \quad (7)$$

(Mavko et al. 2009).

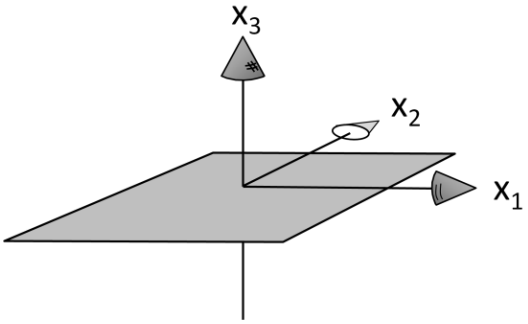

Figure 3: Coordinate system for stiffness matrix.

Also, because of symmetry, $E_{33}\ v_{13} = E_{11}\ v_{31}$. The remaining four are the independent elastic parameters. We identify them as $E_v \equiv E_{33}$, $E_h \equiv E_{11}$, $v_v \equiv v_{31}$ and $v_h \equiv v_{12}$. Here, the subscripts –v‖ and –h‖ denotes –vertical‖ and –horizontal‖, respectively. Please also note that the stiffness parameters C_{44} or C_{55} do not appear directly in the above expressions for Young‘s moduli or the Poisson‘s ratios in a VTI medium, as they do in an isotropic medium. Also, the bounds of the Poisson‘s ratios in the VTI medium are different (Christensen, 2005).

The definitions of Thomsen's VTI anisotropy parameters to be used here are:

$$\delta = ((C_{13}+C_{55})^2 - (C_{33}-C_{55})^2)/ (2C_{33} (C_{33}-C_{55}), \quad (8)$$

$$\varepsilon = ((C_{11}-C_{33})/2C_{33}), \quad (9)$$

$$\gamma = ((C_{66}-C_{55})/2C_{55}. \quad (10)$$

Then, the five normalized elastic parameters can be written as follows:

$$C'_{33} \equiv C_{33}/ C_{33} = 1 \quad (11)$$

$$C'_{55} \equiv C_{55}/C_{33} \equiv \quad (12)$$

$$C'_{66} \equiv C_{66}/C_{33} = \quad (1+2\ ) \quad (13)$$

$$C'_{11} \equiv C_{11}/C_{33} = 1+2 \quad (14)$$

$$C'_{13} \equiv C_{13}/C_{33} = \sqrt{(1-\xi^2)^2 + 2\delta(1-\xi^2)} - \xi^2 \quad (15)$$

$$C'_{12} \equiv C_{12}/ C_{33} = 1+2\varepsilon - 2\xi^2(1+2\gamma). \quad (16)$$

We used the parameter for the square of isotropic velocity or impedance ratio V_s / V_p or I_s / I_p:

$$\xi^2 \equiv C_{55} / C_{33} = (I_s / I_p)^2. \quad (17)$$

Relations 11-17 can then be substituted in the expressions for the Young's moduli and Poisson's ratios, 3-7, to have these elastic parameters explicitly expressed in terms of the anisotropy parameters ε, δ, and γ and the velocity ratio parameter ξ. For the sake of compactness, we keep the normalized C'_{ij} notations and write the four elastic parameters as follows:

$$E_v = C'_{33} - 2C'^2_{13} / (C'_{11} + C'_{12}) \quad (18)$$

$$E_h = C'_{11} + \{(C'^2_{13} (C'_{12} - C'_{11}) + C'_{12} (C'^2_{13} - C'_{12} C'_{33})\} / (C'_{33} C'_{11} - C'^2_{13}) \quad (19)$$

$$v_v = C'_{13} / (C'_{11} + C'_{12}) \quad (20)$$

$$v_h = (C'_{33} C'_{12} - C'^2_{13}) / (C'_{33} C'_{11} - C'^2_{13}). \quad (21)$$

Another elastic parameter of great importance in initiation of fractures through hydraulic stimulation (Higgins, et al., 2008) is the ratio of horizontal stress to vertical stress. Its contribution from the uniaxial stress in a VTI medium is (Thomsen, 1986):

$$K_0 = \sigma_h/\sigma_v = C_{13}/C_{33} = C'_{13}. \quad (22)$$

For an isotropic medium, $K_0 = 1 - 2\xi^2$

No approximations have been invoked so far. One approximation that greatly simplifies the equations is the one linear-in-anisotropy parameters. Then, through simple algebraic manipulation, we can write:

$$C'_{13} \approx 1 - 2\xi^2 + \delta, \text{ and} \quad (23)$$

$$E_v \approx E_0 - 4\nu_0 \delta + 4\nu^2_0 (\varepsilon - \xi^2\gamma)) \quad (24)$$

$$E_h \approx E_0 (1 + \frac{\varepsilon - (1-2\xi^2)\delta}{2\xi^2(3-4\xi^2)(1-\xi^2)} + \frac{4(1-2\xi^2)\gamma}{(3-4\xi^2)}) \quad (25)$$

$$\nu_v \approx \nu_0 \left\{1 + \frac{\delta}{1-2\xi^2} - \frac{2(\varepsilon-\xi^2\gamma)}{1-\xi^2}\right\} \quad (26)$$

$$\nu_h \approx \nu_0 \left(1 + \frac{\varepsilon}{2\xi^2(1-2\xi^2)(1-\xi^2)} - \frac{2\gamma}{(1-2\xi^2)} - \frac{\delta}{(1-\xi^2)}\right) \quad (27)$$

and

$$\sigma_h/\sigma_v = (E_h/E_v)(\nu_v/(1-\nu_h)) = C_{13}/C_{33} \approx 1-2\xi^2 + \delta. \quad (28)$$

Results and Discussion

In Figures 4-7, we show the effects of anisotropy parameters ε, δ, and γ on vertical and horizontal Young's moduli and the Poisson's ratios. These are based on the exact equations, 11-16. The effects are quite dramatic. The vertical Poisson's ratio significantly decreases with ε while the horizontal Poisson's ratio increases. On the other hand, both of the Young's moduli increase with ε. The anisotropy parameter γ has a completely different type of effect—the horizontal Young's modulus initially increases, reaches a maximum, and then falls with further increase in γ. The vertical and horizontal Poisson's ratios show opposite effects with γ.

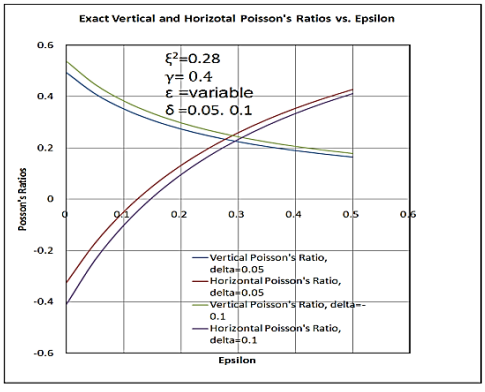

Figure 4: Exact vertical and horizontal Poisson's ratios as a function of ε and for two different values of δ.

The uniaxial stress ratio is dependent only on the δ anisotropy parameter and the square of the vertical velocity ratio (Figure 6), opposing each other.

The results of the approximate equations 24-28 provide the

general trends—the effects seen in Figures 4-7 can be explained through these linear-in-anisotropy equations. However, in terms of the magnitude, they are poor representations of the exact results. These are shown in Figures 8 and 9. Unless the anisotropy is low ~ 0.1, we recommend using the exact expressions.

In Figure 10, we show a set of data points for the stress ratio on shale formations obtained by Jones and Wang (1981), Hornby (1994), Johnston and Christensen (1995), and Wang (2002). We show that these data points representing various shales, fall within a rather restricted range of delta values -0.06-0.15.

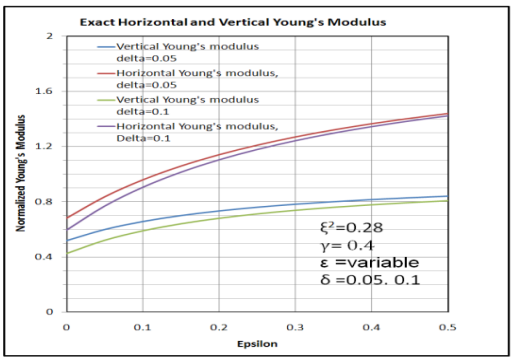

Figure 5: Exact vertical and horizontal Young‘s moduli as a function of ε and for two different values of δ.

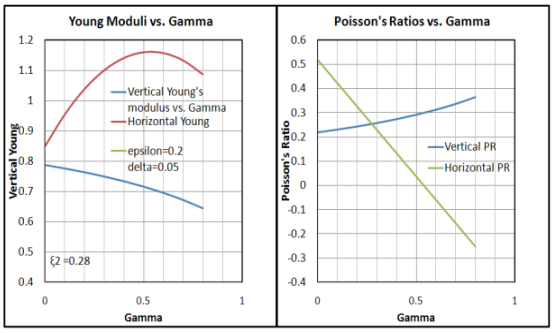

Figure 6: Exact vertical and horizontal Young‘s moduli and Poisson‘s ratios as a function of γ for constant ε and δ.

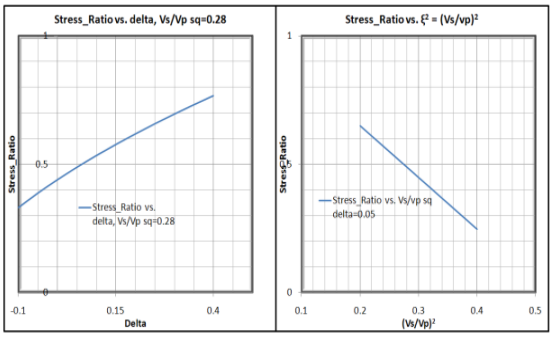

Figure 7: Elastic component of stress ratio as a function of δ and as square of velocity ratio.

Seismic strategy

We showed that anisotropy has significant effects on the two key elastic parameters—the Young‘s modulus and the Poisson‘s ratio. In fact there are two Young‘s moduli and at least two Poisson‘s ratios and they vary significantly with the magnitudes of the anisotropy parameters ε, δ, and γ. Moreover, the uniaxial elastic component of the stress ratio depends strongly on δ. Therefore, these anisotropy parameters must be taken into account to properly characterize any shale reservoir.

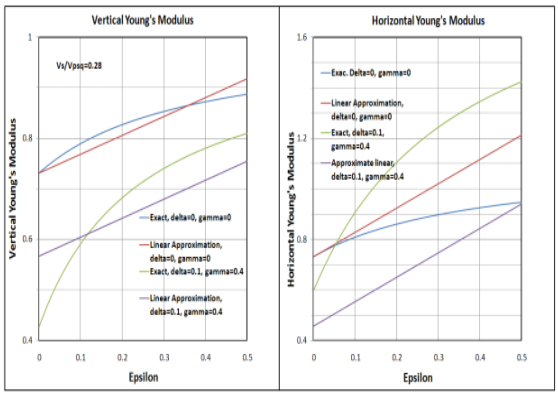

Figure 8: Comparison of exact results with those of linear-in-anisotropy approximations.

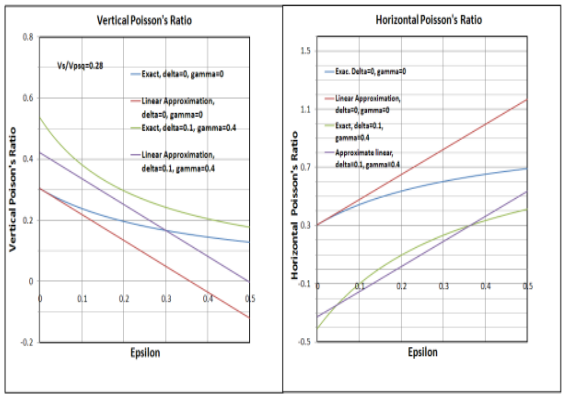

Figure 9: Comparison of exact results of Poisson's ratios with those of linear-in-anisotropy approximations.

Can the P-wave surface seismic measurements alone do it? We need to know vertical P-wave and S-wave velocities and three anisotropy parameters. With high-quality and high-resolution surface seismic data, we can reasonably estimate δ and ε (See Bakulin et al., 2010), and for the remaining parameters, we must depend on the downhole data—wire-line measurements including sonic scanner and borehole seismic such as walkaway vertical seismic profiling. Laboratory experiments on core samples will be also beneficial to obtain valid empirical relationships among some of the parameters to develop a starting model.

We thus propose a prestack full-waveform AVO inversion in a VTI medium constraining elastic parameters based on depth-velocity analysis of P-wave surface seismic data and other information as available. A schematic workflow is shown in figure 11.

Also, the Young's moduli and the Poisson's ratios the drillers must have are the static moduli, not the dynamic moduli estimated through seismic experiments. Presently, the relationship between the two is obtained through laboratory measurements. The dynamic Young's moduli can be larger than the static moduli by a factor of 2 and it may vary from basin to basin.

The initial model can be updated through additional drilling and micro-seismic monitoring, initial production, estimated ultimate recovery data. A schematic workflow for integrating seismic with borehole and other measurements is shown in Figure 11.

Acknowledgement

The authors benefitted from discussions with Colin Sayers and David Padock of Schlumberger Data Consulting and Solutions and WesternGeco, respectively.

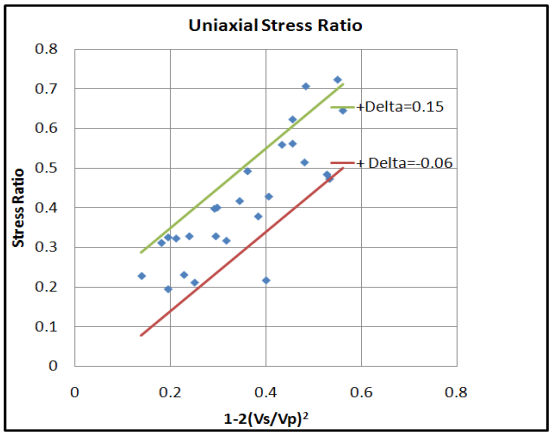

Figure 10: Elastic component of stress ratio as a function 1- 2* $(Vs/Vp)^2$ for various experimental data in ayers (2010), showing that most data points fall between δ= -0.06-0.15.

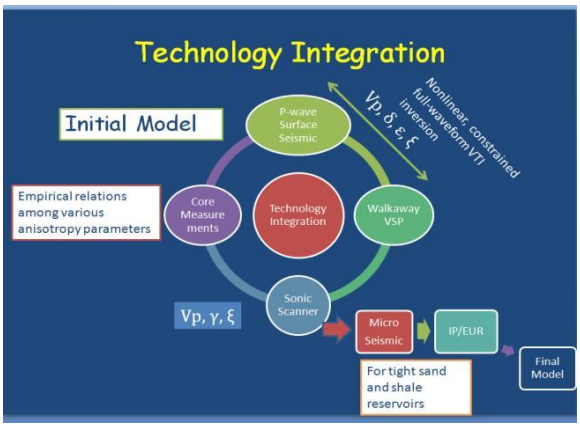

Figure 11: A schematic workflow for shale gas reservoir characterization, integrating surface seismic with borehole and other measurements.

References

Banik, N., C., 1984, Velocity anisotropy in shales and depth estimation in the North Sea Basin: Geophysics, **49**, 1411–1419.

Banik, N., C., A. Koesoemadinata, and K. G. El-Kaseeh, 2010, Young's modulus from single-sensor surface seismic data: 80th Annual International Meeting, SEG, Expanded Abstracts, 2794-2798.

Bakulin, A., Woodward, M., Nichols, D., Osypov, K., and Zdraveva O., Localized anisotropic tomography with well information in VTI media, Geophysics **75**, D37 (2010).

Christensen, R., M. 2005, Mechanics of composite materials, Dover Publications, New York.

Higgins, S., S. Goodwin, A. Donald, T. Bratton, and Tracy George, 2008, Anisotropic Stress Models Improve Completion Design in the Baxter Shale, SPE 115736, 1-10

Hornby, B. E., 1994, The elastic properties of shales: Ph.D. thesis, University of Cambridge.

Johnston, J.E., and N.I. Christensen, 1995, Seismic anisotropy of shales: Journal of Geophysical Research — B: Solid Earth and Planets, **100**, 5991–6003.

Jones, L.E. A., and H. F. Wang, 1981, Ultrasonic velocities in Cretaceous shales from the Williston Basin: Geophysics, **46**, 288–297.

Mavko, G., T. Mukerji, and J. Dvorkin, 2009, The rock physics handbook—tools for seismic analysis in porous media, the Cambridge University Press, Cambridge, UK.

Sayers, C. M., 2010, SEG/EAGE Distinguished Instructor Short Course, Geophysics Under Stress: Geomechanical Applications of Seismic and Borehole Acoustic Waves, Chapter 8, 106-121.

Thomsen, L., 1986, Weak elastic anisotropy: Geophysics, 51, 1954–1966.

Wang, Z., 2002, Seismic anisotropy in sedimentary rocks: Part 2 — Laboratory data: Geophysics, 67, 1423–1440.